

University of Wollongong
Research Online

Australian Institute for Innovative Materials -
Papers

Australian Institute for Innovative Materials

1-1-2015

Effect of tensile load on the actuation performance of pH-sensitive hydrogels

Sina Naficy
University of Wollongong, snaficy@uow.edu.au

Geoffrey M. Spinks
University of Wollongong, gspinks@uow.edu.au

Follow this and additional works at: <https://ro.uow.edu.au/aiimpapers>

 Part of the [Engineering Commons](#), and the [Physical Sciences and Mathematics Commons](#)

Recommended Citation

Naficy, Sina and Spinks, Geoffrey M., "Effect of tensile load on the actuation performance of pH-sensitive hydrogels" (2015). *Australian Institute for Innovative Materials - Papers*. 1285.
<https://ro.uow.edu.au/aiimpapers/1285>

Research Online is the open access institutional repository for the University of Wollongong. For further information contact the UOW Library: research-pubs@uow.edu.au

Effect of tensile load on the actuation performance of pH-sensitive hydrogels

Abstract

pH-responsive hydrogels are capable of converting chemical energy to mechanical work. To optimize their use as actuators, their response when operating against an external load must be fully characterized. Here, the actuation strain of a model pH-sensitive hydrogel as a function of different constant loads is studied. The experimental actuation strain, produced by switching the pH from 2 to 12, decreases significantly and monotonically with increasing initial tensile load. Two models are developed to predict the actuation strain as a function of applied stress. Simple mechanical models based on the change in hydrogel modulus and cross sectional area due to the change in pH are unsatisfactory as they predict only a small change in actuation strain with increasing external stress. However, the model based on the elastic and mixing free energy functions derived from the Flory-Huggins theory is found to accurately account for the actuation strain as a function of stress.

Keywords

actuation, hydrogels, sensitive, effect, load, tensile, ph, performance

Disciplines

Engineering | Physical Sciences and Mathematics

Publication Details

Naficy, S. & Spinks, G. M. (2015). Effect of tensile load on the actuation performance of pH-sensitive hydrogels. *Journal of Polymer Science Part B: Polymer Physics*, 53 (3), 218-225.

Effect of Tensile Load on the Actuation Performance of pH-Sensitive Hydrogels

Sina Naficy, Geoffrey M Spinks

School of Mechanical, Materials and Mechatronic Engineering, Intelligent Polymer Institute and ARC Centre of Excellence for Electromaterials Science, University of Wollongong, Wollongong, NSW 2522, Australia

Correspondence to: Geoffrey Spinks (E-mail: gspinks@uow.edu.au)

ABSTRACT

pH-responsive hydrogels are capable of converting chemical energy to mechanical work. To optimize their use as actuators, their response when operating against an external load must be fully characterized. Here, the actuation strain of a model pH-sensitive hydrogel as a function of different constant loads is studied. The experimental actuation strain, produced by switching the pH from 2 to 12, decreases significantly and monotonically with increasing initial tensile load. Two models are developed to predict the actuation strain as a function of applied stress. Simple mechanical models based on the change in hydrogel modulus and cross sectional area due to the change in pH are unsatisfactory as they predict only a small change in actuation strain with increasing external stress. However, the model based on the elastic and mixing free energy functions derived from the Flory-Huggins theory is found to accurately account for the actuation strain as a function of stress.

KEYWORDS: Hydrogel; Actuator; Stimuli-Responsive; Mechanical Properties; Thermodynamics

INTRODUCTION

Stimuli-responsive materials capable of performing work by converting an external stimulation into mechanical motion are the framework of the evolving field of smart actuators. These materials can be used for different applications, such as artificial muscles,¹ fluid pumps,² valves and gates.³ Piezoelectric materials,⁴ electroactive polymers,⁵ shape memory alloys,⁶ dielectric elastomers⁷ and stimuli-responsive hydrogels are examples of such materials. Hydrogels are known to respond to a variety of external stimuli, including pH,⁸ temperature,⁹ chemical composition of the solvent,¹⁰ ionic strength^{11,12} and electric field.^{13,14} Mechanical properties of hydrogels (especially their stiffness) resemble

those of biological tissue, while the stroke generated is one of the highest amongst actuator materials. The origin of actuation in hydrogels is considered to be the change in their water swelling ratio, as water is absorbed into or exuded out of the hydrogel in response to the stimulation. This volume change can easily be converted into large strokes. When actuation is only the result of free swelling/shrinking, the free actuation strain ε_o can be directly related to the change in the volumetric swelling ratio of the hydrogel before and after stimulation (q_1 and q_2 , respectively) by: $\varepsilon_o \approx (q_2/q_1)^{1/3} - 1$. This simple relationship is valid only when the hydrogel swells/shrinks isotropically and freely with no external

load/constraints being applied. From a practical point of view, however, actuators always operate against an applied load and it is important to understand the effect of load on the actuation performance of actuators.

According to Spinks and Troung,¹⁵ the effect of applied load on the actuation performance of materials is correlated to the change that occurs in the elastic modulus E during the course of actuation. Thus, the stroke generated by hydrogels as a result of stimulation can either be hindered or amplified when an external load is applied, depending on the effect of stimulation on the elastic modulus. While it was shown that the elastic modulus of almost all actuator materials changes during actuation,^{15,16} this change can be particularly dramatic for stimuli-responsive hydrogels. In simple terms, the elastic modulus of a hydrogel can be related to its swelling ratio q by the relation: $E \propto q^{-1/3}$.¹⁷ Since the swelling ratio q of hydrogels changes in response to stimulation (q_1 and q_2 , before and after stimulation), the hydrogel's modulus ratio before and after stimulation is $E_2/E_1 \approx (q_1/q_2)^{1/3}$. This relationship suggests a modulus change of up to 25 % during actuation when swelling ratio varies by a factor of 2.

The effect of applied load and external constraints on the swelling ratio¹⁸ and strain¹⁹ of swollen polymeric networks has also been studied thermodynamically. Generalized expressions were theoretically developed and experimentally tested to study the swelling/shrinking of polymer gels and their kinetics where no external force/constraint was applied.²⁰⁻²² Amongst others, Suo *et. al.* have developed theories for swollen networks²³⁻²⁵ to illustrate the effect of applied load or constraints on the gels.

In the current study, we seek to understand the effect of applied load on the tensile actuation strain of a model pH-sensitive hydrogel actuator. Such studies are difficult since conventional hydrogels are mechanically brittle

and unable to sustain external tensile loads without internal damage. Moreover, the lack of sufficient mechanical properties in submerged hydrogel actuators is a great obstacle in practically utilizing the large deformations that can be generated by these systems. To tackle this problem, we have recently developed a novel pH-sensitive hydrogel based on poly(acrylic acid) (PAA) and polyurethane (PU) with enhanced mechanical performance.²⁶ It was shown that this hydrogel could retain its mechanical integrity during multiple cycles of loading and unloading. In the present study, we used a similar pH-sensitive hydrogel as a model system to conduct a series of actuation experiments by applying different constant loads on the submerged hydrogels while switching the pH. A correlation was established between the actuation strain of the hydrogel under different applied loads with the elastic modulus and swelling ratio before and after stimulation. Two different approaches were considered to model the experimental results. In the *mechanics models*, the general concept initially developed by Spinks and Troung¹⁵ was used to specifically predict the effect of load on the hydrogel actuation through modulus change during the pH switching using Hooke's law and rubber elasticity. In the *thermodynamics model*, Flory-Huggins energy function²⁷ was used as the platform to calculate the effect of pH on the hydrogel strain under an applied load.

Background

I. Mechanics Models

Following Spinks and Troung,¹⁵ here we consider the actuation of a pH-sensitive hydrogel under a constant extensional load f while pH changes from pH_1 to pH_2 . When no load is applied, the volume of dry network is v_d , and the volume of fully swollen hydrogel equilibrated at pH_1 and pH_2 is, respectively, $v_{o,1}$ and $v_{o,2}$. Figure 1 illustrates an example of such a hydrogel, where $\text{pH}_1 < \text{pK} < \text{pH}_2$ and $v_{o,1} < v_{o,2}$, i.e. the hydrogel expands when pH increases from pH_1 to pH_2 .

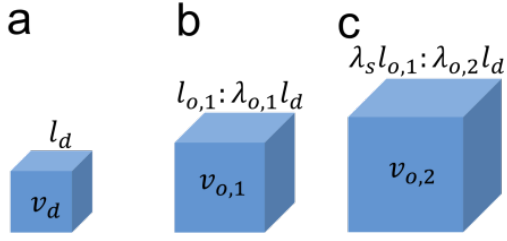


FIGURE 1 Schematic diagram of unconstrained free swelling of a pH-sensitive gel: (a) dry state; (b) hydrogel equilibrated at pH_1 ; (c) hydrogel equilibrated at pH_2 . Swelling is considered to be isotropic.

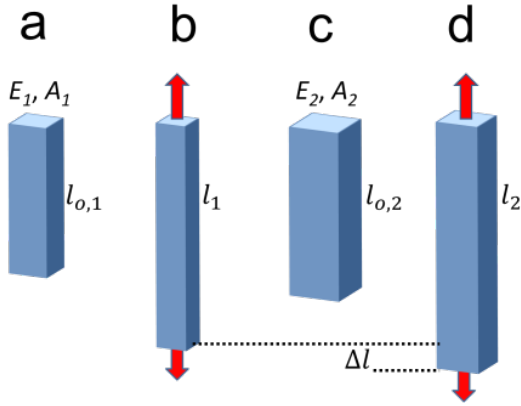


FIGURE 2 Schematic illustration of a tensile hydrogel actuator: (a) hydrogel equilibrated at pH_1 , no load applied; (b) hydrogel shown in (a) subjected to a load at pH_1 ; (c) hydrogel equilibrated at pH_2 , no load applied; (d) hydrogel shown in (c) subjected to the same load as in (b) at pH_2 . Modulus and cross sectional area are E_1 and A_1 in (a) and (b), and E_2 and A_2 in (c) and (d).

According to Figure 1, when no force is applied the dry network expands isotropically by a factor of $\lambda_{o,1}$ (or $\lambda_{o,2}$) in all directions, relative to its dry state, upon equilibrium at pH_1 (or pH_2). Consequently, the isotropic swelling extension in any one direction when pH switches from pH_1 to pH_2 is defined as: $\lambda_s = (v_{o,2}/v_{o,1})^{1/3}$. While for the example illustrated in Figure 1, λ_s is assumed to be larger than 1 (expansion), the derivations presented below are not limited to

an expanding hydrogel and are valid for any λ_s . Under a constant load (Fig. 2), the ultimate actuation strain ε_a generated by the pH change is defined as follows:

$$\varepsilon_a = \frac{\Delta l}{l_{o,1}}. \quad (1)$$

Here, Δl is the length change due to actuation and $l_{o,1}$ is the initial length of the hydrogel equilibrated at pH_1 when no force is applied (initial stage). The basic assumption to determine ε_a in the mechanics models is to ignore any possible effect of load on the stimulation-induced volume change. This assumption allows us to separately treat the effect of load on the length of hydrogel once equilibrated at pH_1 [Fig. 2(a,b)] and then equilibrated at pH_2 [Fig. 2(c,d)]. The swelling/shrinking extension λ_s is defined as:

$$\lambda_s = l_{o,2}/l_{o,1}, \quad (2)$$

where $l_{o,1}$ and $l_{o,2}$ are the length of hydrogel equilibrated at, respectively, pH_1 and pH_2 under no force. The behavior of hydrogel under load can be captured by Hooke's law or from rubber elasticity theory. First, we consider linear elasticity to determine mechanical behavior of the hydrogel actuator. After the load is applied on the hydrogel [Fig. 2(b,d)], the generated strains at pH_1 and pH_2 can be estimated using Hooke's law

$$\varepsilon_i = \sigma_i/E_i, \quad (3)$$

where E_i and σ_i are, respectively, the elastic modulus and applied stress at pH_1 or pH_2 ($i: 1, 2$). The strains ε_i are defined based on the length of hydrogel before and after the application of load ($l_{o,i}$ and l_i , respectively):

$$\varepsilon_i = \frac{l_i - l_{o,i}}{l_{o,i}}. \quad (4)$$

By inserting Eq. (4) in Eq. (3) and using Eq. (2) to eliminate $l_{o,2}$, the final lengths of hydrogel

under the load and equilibrated at pH₁ and pH₂ are obtained:

$$l_1 = \left(\frac{\sigma_1}{E_1} + 1\right) l_{o,1}, \quad (5a)$$

$$l_2 = \left(\frac{\sigma_2}{E_2} + 1\right) \lambda_s l_{o,1}. \quad (5b)$$

The lengths of hydrogel under applied load at pH₁ and pH₂ [Eq. (5)] are then used in Eq. (1), which leads to a generic expression for the actuation strain:

$$\varepsilon_a = \left(\frac{\sigma_2}{E_2} + 1\right) \lambda_s - \left(\frac{\sigma_1}{E_1} + 1\right). \quad (6)$$

Since $\sigma_i = f/A_i$ (A_i denotes the unloaded cross-sectional area at pH₁ or pH₂ for i : 1, 2), the tensile stress at constant force will depend on the network swelling/shrinking. In materials where small volume changes occur, like conducting polymers, the cross-sectional area could be assumed to be constant.¹⁵ However, for hydrogels where large swelling ratio changes take place during actuation, this assumption is not valid anymore. In this case, while the applied load remains constant during the actuation, the cross-section of hydrogel is considered to expand/contract isotropically with the rest of hydrogel.²⁸ The change in cross-sectional area from A_1 before stimulation to A_2 after stimulation can be asserted by: $A_2 = \lambda_s^2 A_1$ so that:

$$\varepsilon_a = (\sigma_1/E_1) \left[\frac{1}{\lambda_s(E_2/E_1)} - 1 \right] + (\lambda_s - 1). \quad (7)$$

For all E_2/E_1 and λ_s , Eq. (7) predicts a linear trend for ε_a as a function of σ_1/E_1 . For $E_2/E_1 < \lambda_s^{-1}$, the actuation strain increases with increasing stress. However, a switch-over occurs at $E_2/E_1 = \lambda_s^{-1}$, where for $\lambda_s^{-1} < E_2/E_1$ actuation strain begins to decrease as stress increases. Moreover, Eq. (7) suggests that ε_a

has a decreasing trend as a function of E_2/E_1 , regardless of λ_s , where applied stress can amplify the effect of modulus change. For more detailed discussion see the Supporting Information.

Equation (7) was obtained assuming a Hookean behaviour for hydrogels. However, the polymer chains of a fully swollen network are most likely above their T_g and behaving similar to rubbers, hence the rubber elasticity model seems to be more relevant to model the mechanical performance of the gel network. From rubber elasticity theory, applied engineering stress (σ_i) is related to the stress induced extension ratio (λ_i) by:

$$\sigma_i = G_i \left(\lambda_i - \frac{1}{\lambda_i^2} \right), \quad (8)$$

where G_i is shear modulus at the respective state (i : 1, 2). The extension ratios are based on the initial length of fully swollen network at each pH, and the following relationships are assumed between applied stresses and moduli before and after pH change: $\sigma_2 = \lambda_s^{-2} \sigma_1$ and $G_2 = \lambda_s^{-1} G_1$. Actuation strain is determined from $\varepsilon_a = \lambda_s \lambda_2 - \lambda_1$. For various values of λ_s , Figure 3(a) shows actuation strain plotted as a function of normalized stress (σ_1/E_1).

For both an expanding and a contracting hydrogel, the actuation strain decreases as applied stress increases [Fig. 3(a)]. The effect of λ_s on the actuation strain is highlighted in Figure 3(b), where all composing components of ε_a are plotted against λ_s for $\sigma_1/E_1=1$. Interestingly, λ_2 decreases as λ_s increases, regardless of λ_s , although this decreasing trend is more prominent when $\lambda_s < 1$. However, the multiplication of λ_2 and λ_s results into a gradual increase in $\lambda_s \lambda_2$ with λ_s . Therefore, the overall actuation strain ($\varepsilon_a = \lambda_s \lambda_2 - \lambda_1$) slightly increases with λ_s , suggesting a trend contrary to those predicted by Hooke's law (See Supporting Information).

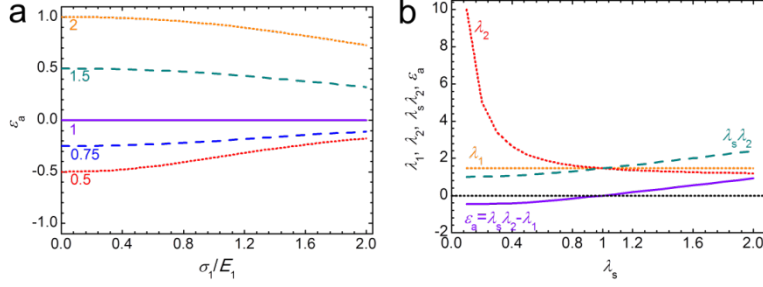


FIGURE 3 (a) Actuation strain ϵ_a vs. normalized stress σ_1/E_1 [based on rubber elasticity theory: Eq. (8)] for various λ_s as indicated on each curve. (b) Effect of λ_s on λ_1 , λ_2 , $\lambda_s \lambda_2$ and ϵ_a , when $\sigma_1/E_1 = 1$.

II. Thermodynamics Model

In the previous section, the effect of the applied external force on the swelling ratio of pH-sensitive hydrogels was assumed to be negligible. Consequently, the effect of applied load on the actuation strain was considered to be due only to the change in the elastic modulus and cross sectional area. In practice, however, the swelling process in which a polymer network imbibes a large quantity of solvent is markedly affected by the applied load and the interaction between solvent and polymer network. According to Flory²⁷ and many others, the equilibrium swelling of a gel is determined by the combination of network's elastic response and the chemical activity of diluent within the network:

$$W_t = W_e + W_m, \quad (9)$$

where W_t is the total free energy of the system per unit volume in reference state (dry network), and is a function of the number of solvent molecules per unit volume N_s and the extension ratios (i.e. λ_x , λ_y and λ_z) based on dry state of the network. $W_e(\lambda_x, \lambda_y, \lambda_z)$ and $W_m(N_s)$ are, respectively, the elastic and mixing free energy contributions. Equation (9) is generally valid for neutral elastic networks. In the case of a charged network, however, other free energy contributions can be added to the summation presented in Eq. (9):^{25, 27, 29}

$$W_t = W_e + W_m + W_{dis} + W_{ion}. \quad (10)$$

Here, W_{ion} represents the free energy term for the mixing of ions and W_{dis} is the term associated with the change in free energy due to dissociation of the ionic side groups on the polyelectrolyte backbone. In a deformed hydrogel in equilibrium with its surrounding, the nominal normal stresses (force per unit area in the reference state) are written as³⁰

$$\sigma_x = \partial W_t / \partial \lambda_x - (\Pi_{mix} + \Pi_{ion}) \lambda_y \lambda_z, \quad (11a)$$

$$\sigma_y = \partial W_t / \partial \lambda_y - (\Pi_{mix} + \Pi_{ion}) \lambda_x \lambda_z, \quad (11b)$$

$$\sigma_z = \partial W_t / \partial \lambda_z - (\Pi_{mix} + \Pi_{ion}) \lambda_x \lambda_y. \quad (11c)$$

In Eqs. (11), Π_{mix} is the overall osmotic pressure representing the resistance against solvent molecules to enter the network from the outside environment. Π_{ion} is the osmotic pressure in the hydrogel resulted from mobile ions. Both osmotic pressures are a function of hydrogel's swelling ratio.

Assuming the gel volume change is mainly due to the solvent molecules, the extension ratios are related to N_s by

$$1 + v_s N_s \approx \lambda_x \lambda_y \lambda_z. \quad (12)$$

where v_s is the volume of a solvent molecule, N_s is the number of solvent molecules per unit volume of the dry network and $v_s N_s$ is the volume of solvent molecules divided by the volume of the dry network. In Eqs. (11) and

(12), λ_x , λ_y , λ_z and N_s are allowed to vary independently as long as all equations are satisfied. The elastic free energy term in Eqs. (9) and (10) can be determined by a Gaussian-chain model:^{31, 32}

$$W_e = (NkT/2)[(\lambda_x^2 + \lambda_y^2 + \lambda_z^2 - 3) - 2 \ln(\lambda_x \lambda_y \lambda_z)]. \quad (13)$$

Here, N is the number of elastically effective polymer chains per reference volume (dry network). Inserting Eq. (13) in Eqs. (11) results in

$$\sigma_x = NkT(\lambda_x - \lambda_x^{-1}) - (\Pi_{mix} + \Pi_{ion})\lambda_y \lambda_z, \quad (14a)$$

$$\sigma_y = NkT(\lambda_y - \lambda_y^{-1}) - (\Pi_{mix} + \Pi_{ion})\lambda_x \lambda_z, \quad (14b)$$

$$\sigma_z = NkT(\lambda_z - \lambda_z^{-1}) - (\Pi_{mix} + \Pi_{ion})\lambda_x \lambda_y. \quad (14c)$$

For a hydrogel under uniaxial load in the x -direction, the transversal stresses are zero ($\sigma_y = \sigma_z = 0$) and $\lambda_y = \lambda_z$. From Flory-Huggins theory, the mixing osmotic pressure for solvent molecules and long polymer chains can be expressed as^{33, 34}

$$\Pi_{mix} = -\frac{kT}{v_s} \left[\frac{1}{\lambda_x \lambda_y^2} + \ln \left(1 - \frac{1}{\lambda_x \lambda_y^2} \right) + \frac{\chi}{\lambda_x^2 \lambda_y^4} \right], \quad (15)$$

In Eq. (15), χ is a measure of enthalpy of mixing and $\lambda_x \lambda_y^2$ represents the volume swelling ratio of hydrogel. From Eq. (12), it is obvious that $1/\lambda_x \lambda_y^2$ is the dry network volume fraction and $(1 - 1/\lambda_x \lambda_y^2)$ is the solvent volume fraction. Hence, Eq. (15) correlates the mixing osmotic pressure to the hydrogel swelling ratio through the extension ratios of the deformed network, regardless of how the network has been deformed. Ionic osmotic pressure can also be related to the swelling state of the network. It was shown that for a PAA-based hydrogel the ionic osmotic pressure is almost independent of swelling ratio at both very low and very high

pHs. Also, it was found that ionic osmotic pressure is a dominant factor at very high swelling ratios.³⁰ Since in this study the actuation test was operated between a very low pH and a very high pH, we assumed a constant ionic osmotic pressure at each pH. Inserting Eq. (15) into Eqs. (14) results into a set of two non-linear equations as a function of λ_x and λ_y , where the only parameters required to solve these equations are N , χ and Π_{ion} .

EXPERIMENTAL

Sample Preparation

An interpenetrating polymer network system was developed based on poly(acrylic acid) (PAA) and polyurethane (PU). The PU used here was HydroMed™ D3 (AdvanSource, USA), referred to as PU-D3 hereafter. PU-D3 is a hydrophilic, polyether-based PU, soluble in the mixture of ethanol (EtOH) and water, but insoluble in water alone. The hydrogels made of PU-D3 were found to be moderately swollen (water content ~60 %) and mechanically robust. Briefly, PU-D3 films were prepared by dissolving the granules in 95:5 mixture of EtOH and Milli-Q water, followed by solution-casting. The solvent was removed by placing the films in the oven (80 °C, overnight). To introduce pH sensitivity into the system, the PU-D3 films were transferred into an aqueous solution of acrylic acid (AA; Sigma-Aldrich) monomer solution. The monomer solution was made of AA monomer (17.5 % w/w), N,N'-methylenebisacrylamide crosslinker (Sigma-Aldrich) (0.34 mol% based on AA) and α -ketoglutaric acid UV-initiator (Sigma-Aldrich) (0.5 mol% based on AA), all dissolved in water. Adequate amount of sodium hydroxide was added to the monomer solution to fully neutralize the AA monomer. The PU-D3 films remained in the AA monomer solution for 2 days then sandwiched between two glass plates. No spacer was used to separate the plates. The PAA network was then formed within the PU-D3 film using UV-initiation polymerization (240 W power, 300 nm

wavelength for 12 hours, fan cooled). PU-D3/PAA hydrogel films were then removed from the mould and stored in Milli-Q water for 1 week prior to further experiments. A similar process for making PU-D3/PAA hydrogels is described elsewhere.²⁶ The main difference between the method employed here and the one reported previously²⁶ is the way PU-D3 films were prepared. In the latter, solvent was removed slowly, under room temperature, followed by exposing the dry PU-D3 films to water.

Actuation Testing and Sample Characterization

Samples for mechanical and actuation testing were prepared by cutting hydrogels into ribbons (7.0 mm×3.5 mm×0.5 mm, fully swollen in water). The ends of hydrogel ribbons were then fixed between plastic films using superglue, with one end attached to ultra-high molecular weight polyethylene fishing lines while the other end was fixed to the bottom of plastic tubes. The fishing line was used to connect the hydrogel ribbons to the testing device [Fig. 4(a)].

Actuation testing and mechanical properties characterization were performed on fully submerged hydrogels using a dual-mode lever system (305B, Aurora Sci. Inc.). An e-corder (eDAQ) was used as the interface to connect the lever arm to the computer. To measure E_1 and E_2 (modulus of submerged hydrogel equilibrated at, respectively, $pH_1=2$ and $pH_2=12$), the force was ramped from zero to the desired value while displacement was recorded.

The actuation strain of hydrogels was measured where hydrogel films were connected to the lever arm [Fig. 4(b)]. No force was applied on the hydrogels at this point, and hydrogels were allowed to rest at pH_1 for at least 2 days prior to the test. A constant tensile load was applied to the samples while the longitudinal deformation of the hydrogels was recorded over a 10^5 sec time period. After this period, the initial pH solution was drained and immediately replaced by the second pH solution. Again, longitudinal

deformation was recorded while force was kept constant over a period of 10^5 sec. The constant applied load was 30, 40, 60, 90 and 120 mN. For each measurement, a new sample was used and experiments were repeated up to three times with different samples.

Swelling ratio of hydrogels at both pHs was measured by recording the mass and dimension of samples equilibrated at the corresponding pH, followed by measuring the mass and dimensions of fully dried samples. λ_s was also calculated using Eq. (2) when dimension of fully swollen hydrogels equilibrated at pH_1 was measured followed by switching the pH and recording the dimension change over a period of 2 days.

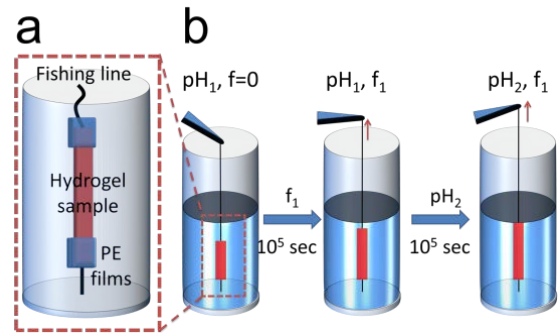


FIGURE 4 Experimental set up: (a) a hydrogel sample is fixed to the bottom of a PE tube where pH solution will be added. Fishing line is used to connect the topside of the hydrogel to the external measuring device (e.g. lever arm); (b) actuation testing set up.

RESULTS AND DISCUSSION

The effect of pH on the modulus of hydrogels was determined for submerged PU-D3/PAA hydrogels equilibrated at $pH_1=2$ and $pH_2=12$. The modulus of hydrogels equilibrated at pH_1 was 294 ± 9 kPa, while hydrogels equilibrated at pH_2 had a modulus of 170 ± 4 kPa. The volumetric swelling ratio of hydrogels at pH_1 and pH_2 was also measured to be, respectively, 2.5 and 10.1. The swelling/shrinking extension

λ_s [Eq. (2)] for switching from pH_1 to pH_2 was measured to be 1.60 ± 0.04 .

Figure 5 presents an example of strain ε (based on the initial unloaded length of hydrogel equilibrated at $\text{pH}_1=2$) as a function of time t when a 30 mN load was applied at $t=0$, followed by pH switch to $\text{pH}_2=12$ at $t=10^5$ sec. The 30 mN load was kept constant during the course of the experiment. Similar to this example, in all cases the hydrogels were already in equilibrium at $\text{pH}_1=2$ at $t=0$ under no force. After the load was applied an immediate response was observed (elastic response), followed by a time-dependent length increase. The time-dependent length change was considered to be due to the poroelastic nature of the hydrogels, where solvent molecules migrated in or out of the network to adjust to the deformation which was rapidly applied.

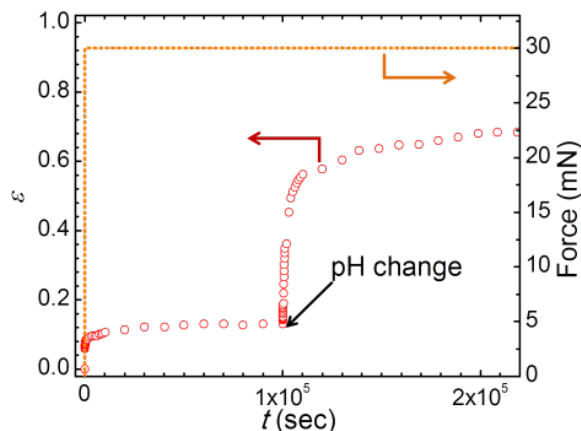


FIGURE 5 Hydrogel strain ε (left axis) as a function of time t , where a 30 mN load (right axis) was applied at $t=0$ and maintained constant over time. pH was changed from pH_1 to pH_2 at $t=10^5$ sec. ε is based on the initial unloaded length of hydrogel equilibrated at $\text{pH}_1=2$.

The actuation strain caused by switching the pH from 2 to 12 was measured using Eq. (1). The experimentally measured moduli (E_1 and E_2) and λ_s were used to calculate the actuation strain as a function of stress, using Eq. (7) for

the mechanics model based on Hooke's law. Similarly, E_1 and E_2 was used to calculate G_1 and G_2 in order to employ Eq. (8) to calculate actuation strain as a function of stress based on the rubber elasticity. In calculating shear modulus a Poisson's ratio of 0.5 was assumed since tensile tests were performed rapidly.

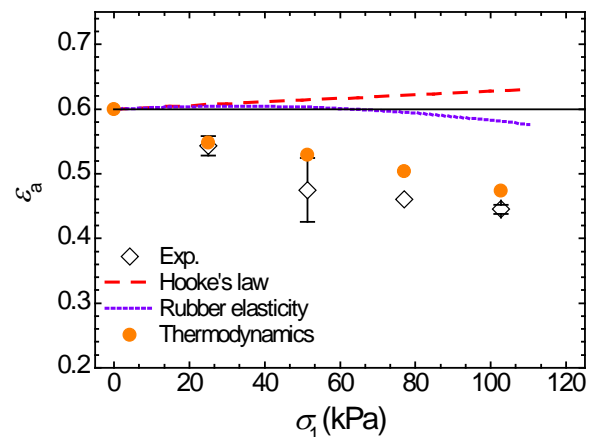


FIGURE 6 Comparison between actuation strains obtained experimentally (open diamonds) and those predicted by the mechanics models based on Hooke's law [Eqs. (7); broken line] and rubber elasticity [Eq. (8); dotted line]. Calculated values obtained from thermodynamics model [Eqs. (14) and (15)] are shown by filled circles. The x-axis represents the nominal stress applied to the hydrogels equilibrated at pH_1 . The solid line indicates the actuation resulted from free swelling when no force is applied. Strains were obtained 10^5 sec after pH change.

The experimental results of actuation strain measurements ε_a are presented in Figure 6 vs. applied stress (open diamonds), along with the calculated values from the Hooke's law [Eq. (7); broken line] and the rubber elasticity model [Eq. (8); dotted line]. In Figure 6, the x-axis represents the nominal stress based on the cross sectional area of the undeformed hydrogel at pH_1 . A significant decrease in the experimentally measured actuation strain was observed with increasing stress. However, none of the mechanics models based on either

Hooke's law or rubber elasticity were able to fit the experimental data. The model based on Hooke's law predicts a slight upward increase in the strain with increasing stress. The rubber elasticity model follows the Hooke's law prediction at small stresses, and then exhibits a decreasing trend at higher stresses, although the predicted actuation strains are considerably higher than experimental results.

To determine actuation strain using the thermodynamics model based on Eqs. (14) and (15), N , χ and Π_{ion} are required. N is the number of elastically effective chains in the network and can be determined from hydrogel's modulus. According to rubber elasticity theory, the shear modulus of a network G_i can be related to the swelling ratio ($\lambda_{o,i}^3$) by:

$$G_i = \frac{NkT}{\lambda_{o,i}}. \quad (16)$$

The hydrogel's modulus was measured experimentally for pH₁ and pH₂. Using Eq. (16), estimated N for pH₁ and pH₂ were, $3.31 \times 10^{25} \text{ m}^{-3}$ and $3.06 \times 10^{25} \text{ m}^{-3}$, respectively. Although the higher N at pH₁ can be explained by possible hydrogen bonding formation between hydrogenated carboxylic groups of PAA and ethylene glycol units of polyurethane backbone in acidic pHs, we assumed a constant N at both pHs. Hence, the average value of $3.18 \times 10^{25} \text{ m}^{-3}$ was used as N in calculating actuation strains. In Eqs. (14) and (15), other parameters are $v_s \sim 10^{-29} \text{ m}^3$ as a representative volume of a water molecule and $kT \sim 4 \times 10^{-21} \text{ J}$ (room temperature). Both χ and Π_{ion} were set as fitting parameters. Equations (14) and (15) can be solved for any given σ_x (applied stress based on dry state) with a set of χ and Π_{ion} , once for pH₁ and then for pH₂ to determine $\lambda_{x,1}$ and $\lambda_{x,2}$ (extension ratios at pH₁ and pH₂ based on dry state). The calculated extension ratios were used to calculate actuation strain from

$$\varepsilon_a = (\lambda_{x,2} - \lambda_{x,1}) / \lambda_{o,1}, \quad (17)$$

where $\lambda_{o,1}$ represents the free swelling extension ratio of hydrogel at pH₁. The actuation strains determined by the thermodynamics model are plotted against applied stress (based on undeformed hydrogel at pH₁), as shown in Figure 6 with filled circles. The fitting parameters used to obtain these results are $\chi = 0.499$ and $\Pi_{ion} = 5.1 \text{ kPa}$ for pH₁ and $\chi = 0.491$ and $\Pi_{ion} = 4.5 \text{ kPa}$ for pH₂. The values obtained here for the Flory-Huggins parameter χ are in agreement with those given for crosslinked poly(acrylamide) hydrogels swollen in water (0.49-0.51).³⁵ The ionic osmotic pressures Π_{ion} are also in the same range as those calculated for poly(acrylic acid-co-acrylamide) gels swollen at various pHs (1-4 kPa).³⁰ Unlike the mechanics models, the thermodynamics model fits the experimental results nicely. Comparing the thermodynamics model with rubber elasticity, the thermodynamics model has additional energy terms that account for the osmotic pressures that appeared in Eqs. (14). Contrary to rubber elasticity theory where the volume remains constant under applied load, the thermodynamics model allows for additional volume change when the network is subjected to the load.

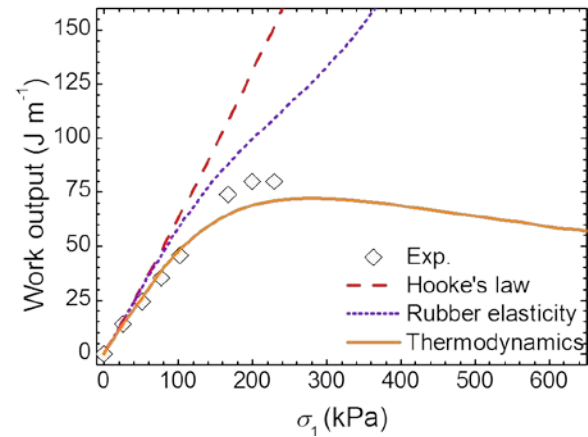


FIGURE 7 Work output normalized to the unit length of the actuator as a function of applied stress.

The mechanical work per unit length of actuator performed by changing the pH while load is

constant was estimated as $F \times \varepsilon_a$. Results are illustrated in Figure 7 as work output as a function of applied stress for the mechanics models based on Hooke's law (broken line), and rubber elasticity (dotted line) along with the thermodynamics model (solid line) and the experimental data (diamonds). The difference in trends is noticeable between Hooke's law, rubber elasticity and the thermodynamics model. Since Hooke's law is based on linear elasticity with a gradual increase in actuation strain as a function of applied stress, the predicted work output, too, linearly increases with stress. The work output predicted from rubber elasticity matches the Hooke's law prediction at small stresses, then deviates from the Hooke's law curve at higher stresses as a result of the lower predicted strains. The thermodynamics prediction for work output, however, differs from the mechanics models, exhibiting a maximum around ~ 200 kPa, where work output decreases with further increasing the applied stress. Clearly, the thermodynamics model fits the experimental data very well and was further evaluated by conducting additional actuation experiments at higher stresses. Here the work output reaches a peak, but is slightly higher than the thermodynamic model predictions. The underestimation of the work output can be attributed to a small amount of non-recoverable creep strain that becomes more significant as stress increases. This suggests that, based on experimental observations and the thermodynamics model, there must exist an optimum stress in which a pH sensitive actuator can operate to generate the maximum work output.

CONCLUSIONS

A pH-sensitive hydrogel was created based on polyurethane and poly(acrylic acid). The effect of applied load on the actuation performance of this hydrogel was studied by measuring the actuation strain of hydrogels under different constant forces. Hydrogel ribbons equilibrated at $\text{pH}_1=2$ were subjected to 30 mN, 60 mN, 90

mN and 120 mN loads for 10^5 sec, followed by a pH switch to $\text{pH}_2=12$ for another 10^5 sec. The deformation of hydrogels was recorded over time. It was found that the pH-stimulated actuation strain of the hydrogel gradually decreases as applied load increases. Two different approaches were used to model the measured actuation strain of hydrogels, namely, the mechanics models and the thermodynamics model. In the former approach, the change in modulus and cross sectional area of hydrogels due to pH change were taken into account to predict the actuation strain. The mechanics models were formulated based on Hooke's law and rubber elasticity theory. In the thermodynamics approach, measured Young's modulus of hydrogels and their swelling ratios at pH_1 and pH_2 were used to calculate the actuation strains using thermodynamics derivations based on the free energies of network and its environment. It was found that the thermodynamics model is able to fit the experimental actuation strains as a function of applied stress very well. On the other hand, the mechanics models were unsatisfactory: the model based on Hooke's law predicted a slight increase in the actuation strain, while the model based on rubber elasticity followed Hooke's law model at lower stresses then began to decrease with further increasing of stress. Work output was calculated based on these three models and compared with experimental results. Both mechanics models based on Hooke's law and rubber elasticity predicted that work output increases continuously with applied stress, while the thermodynamics model followed the experimental results, and exhibited a peak in work output as a function of applied stress.

ACKNOWLEDGEMENTS

The authors acknowledge financial support through the University of Wollongong's Global Challenges Program and the Australian Research Council's Centres of Excellence and Professorial Fellowship programs.

REFERENCES AND NOTES

1. D. Brock, W. Lee, D. Segalman, W. Witkowski, *J. Intel. Mat. Syst. Str.* **1994**, *5*, 764-771.
2. L. Dong, H. Jiang, *Soft Matter* **2007**, *3*, 1223-1230.
3. D. J. Beebe, J. S. Moore, Q. Yu, R. H. Liu, M. L. Kraft, B.-H. Jo, C. Devadoss, *Proc. Natl. Acad. Sci.* **2000**, *97*, 13488-13493.
4. E. F. Crawley, J. De Luis, *AIAA J.* **1987**, *25*, 1373-1385.
5. Electroactive Polymer Actuators as Artificial Muscles; Y. Bar-Cohen, Ed.; SPIE Press: Washington, **2004**.
6. R. C. O'Handley, *J. Appl. Phys.* **1998**, *83*, 3263-3270.
7. P. Brochu, Q. Pei, *Macromol. Rapid Commun.* **2010**, *31*, 10-36.
8. Q. Yu, J. M. Bauer, J. S. Moore, D. J. Beebe, *Appl. Phys. Lett.* **2001**, *78*, 2589-2591.
9. M. E. Harmon, M. Tang, C. W. Frank, *Polymer* **2003**, *44*, 4547-4556.
10. T. Tanaka, D. Fillmore, S.-T. Sun, I. Nishio, G. Swislow, A. Shah, *Phys. Rev. Lett.* **1980**, *45*, 1636-1639.
11. V. Kozlovskaya, E. Kharlampieva, M. L. Mansfield, S. A. Sukhishvili, *Chem. Mater.* **2005**, *18*, 328-336.
12. F. Lai, H. Li, *Soft Matter* **2010**, *6*, 311-320.
13. M. L. O'Grady, P.-I. Kuo, K. K. Parker, *ACS Appl. Mater. Interfaces* **2010**, *2*, 343-346.
14. M. J. Bassetti, A. N. Chatterjee, N. R. Aluru, D. J. Beebe, *J. Microelectromech. Syst.* **2005**, *14*, 1198-1207.
15. G. M. Spinks, V.-T. Truong, *Sens. Actuators, A* **2005**, *119*, 455-461.
16. G. M. Spinks, L. Liu, G. G. Wallace, D. Zhou, *Adv. Funct. Mater.* **2002**, *12*, 437-440.
17. M. Rubinstein; R. H. Colby, In *Polymer Physics*; Oxford University Press: New York, **2003**.
18. T. Budtova, I. Suleimenov, *Polymer* **1997**, *38*, 5947-5952.
19. W. R. K. Illeperuma, J.-Y. Sun, Z. Suo, J. J. Vlassak, *Soft Matter* **2013**, *9*, 8504-8511.
20. Y. Li, T. Tanaka, *J. Chem. Phys.* **1990**, *92*, 1365-1371.
21. C. J. Durning, K. N. Morman, *J. Chem. Phys.* **1993**, *98*, 4275-4293.
22. T. Tanaka, D. J. Fillmore, *J. Chem. Phys.* **1979**, *70*, 1214-1218.
23. W. Hong, X. Zhao, J. Zhou, Z. Suo, *J. Mech. Phys. Solids* **2008**, *56*, 1779-1793.
24. W. Hong, Z. Liu, Z. Suo, *Int. J. Solids Struct.* **2009**, *46*, 3282-3289.
25. R. Marcombe, S. Cai, W. Hong, X. Zhao, Y. Lapusta, Z. Suo, *Soft Matter* **2010**, *6*, 784-793.
26. S. Naficy, G. M. Spinks, G. G. Wallace, *ACS Appl. Mater. Interfaces* **2014**, *6*, 4109-4114.
27. P. J. Flory, In *Principles of Polymer Chemistry*; Cornell University Press: Ithaca, **1953**.
28. A. Gestos, P. G. Whitten, G. G. Wallace, G. M. Spinks, *Soft Matter* **2012**, *8*, 8082-8087.
29. J. Ricka, T. Tanaka, *Macromolecules* **1984**, *17*, 2916-2921.
30. J. Li, Z. Suo, J. J. Vlassak, *Soft Matter* **2014**, *10*, 2582-2590.
31. P. J. Flory, *J. Chem. Phys.* **1950**, *18*, 108-111.
32. P. J. Flory, Y.-I. Tatara, *J. Polym. Sci., Part B: Polym. Phys.* **1975**, *13*, 683-702.
33. M. L. Huggins, *J. Chem. Phys.* **1941**, *9*, 440-440.
34. P. J. Flory, *J. Chem. Phys.* **1942**, *10*, 51-61.
35. J. Li, Y. Hu, J. J. Vlassak, Z. Suo, *Soft Matter* **2012**, *8*, 8121-8128.

GRAPHICAL ABSTRACT

Sina Naficy, Geoffrey M Spinks

Effect of Tensile Load on the Actuation Performance of pH-Sensitive Hydrogels

Hydrogels that respond to pH changes can be used as artificial muscles. Here it is shown that the actuation stroke decreases with increasing external tensile stress applied to the hydrogel prior to pH switching. Changes in elastic modulus and cross-sectional area cannot account for this decrease in actuator stroke, however, thermodynamic treatments that involve both mixing and elastic energies can successfully model the observed behavior.

